Effect of Molecular Orientation on the Elastic Constants of Polypropylene

ARTICLE *in* MACROMOLECULES · MARCH 2000

Impact Factor: 5.8 · DOI: 10.1021/ma9906579

3 AUTHORS, INCLUDING:

D. Renusch
General Electric
53 PUBLICATIONS **433** CITATIONS

Macromolecules **2000,** *33,* 1819–1826

Effect of Molecular Orientation on the Elastic Constants of Polypropylene

Sai R. Kumar*,†

Department of Materials Science & Engineering, University of Michigan, Ann Arbor, Michigan 48109-2136

Daniel P. Renusch and Marcos Grimsditch*

Materials Science Division, Argonne National Laboratory, Argonne, Illinois 60439

Received April 27, 1999; Revised Manuscript Received October 26, 1999

ABSTRACT: The Brillouin spectroscopic measurements of elastic properties of polypropylene films fabricated by different processing techniques are described. We find that the elastic symmetry and the associated elastic constants are dependent on the molecular orientation brought about by the processing conditions used to produce the films. We have shown that Brillouin scattering techniques can successfully be used to track the molecular orientation induced by uniaxial stretching. We find a direct correspondence between the Brillouin measurements and optical birefringence measurements, illustrating that molecular orientation plays a dominant role in determining the mechanical anisotropy in these materials.

I. Introduction

The molecular orientation in polymeric materials produced by common processing techniques can be greatly influenced by processing conditions. For example, a hydrostatically extruded specimen of polypropylene exhibits a 10-fold increase in the longitudinal tensile strength at a deformation ratio of 5.5, compared to a billet.[1] Other useful properties of polypropylene such as its outstanding resistance to low-frequency flexing and its good impact strength are also related to the molecular orientation brought about by controlled processing conditions. The study of molecular orientation in polymeric materials is valuable in establishing a correlation of the physical properties with processing conditions.

Anisotropy in the properties of polymer materials can be brought about by either incidental or deliberate processing conditions and can be measured by a variety of techniques.[2] Such an anisotropy is related to the degree of preferential molecular orientation of the polymer molecules. Nondestructive experimental techniques capable of probing the effects of molecular orientation allow a direct correlation of the processing technique to the product morphology. Brillouin scattering, which is the inelastic scattering of light by thermal acoustic phonons, allows a complete characterization of elastic properties of materials through the measurement of hypersonic velocities; it typically probes the sample on a 100 μm scale. The dependence of the sound velocity on the molecular anisotropy has been well established.[3,4] It is the purpose of this paper to illustrate how the molecular orientation brought about by different processing techniques influences the elastic symmetry and the associated elastic constants (as measured by Brillouin spectroscopy) for polypropylene (PP). We chose polypropylene in our study since it is a versatile thermoplastic, which can be fabricated by all four major polymer processing techniques: films, fibers, molded goods, and extruded profiles.

Our elastic constant results are correlated with birefringence and piezobirefringence studies on the same samples, and a model is presented that provides a simple, semiquantitative explanation of both the elastic and optical data as a function of molecular orientation.

II. Experimental Section

Sample Details. The PP samples included in this study were fabricated by different techniques. PP-COMP was compression molded from Amoco PP 5013 resin having a melt flow index of 3.3 dg/min, using a laboratory-scale Carver press, operated with a platen temperature of 220 °C and a maximum pressure of 7000 psi. A uniaxially stretched film, PP-6X, and a biaxially stretched film, PP-BIAX, were obtained from Amoco and were used without further processing. These films were fabricated from extrusion grade Amoco PP (5013 or 6345) with a melt flow index in the range 2.5–4.0 dg/min; process conditions used in their fabrication were unavailable. We obtained three forged PP samples denoted as PP-A0(X), PP-A1(11), and PP-A1(26) from Prof. Porter of the University of Massachusetts. These samples were fabricated from a molded sheet of isotactic PP (Philips Co; resin melt index = 4 dg/min; sheet thickness = 5.6 mm) which was uniaxially and isothermally compressed by a forging process under a steady compression speed of 0.254 cm/min. Different compression draw ratios[5] (given in parentheses as X, 11, and 26 for the samples used in our study; X = unknown) were obtained by adjusting the load; further fabrication details can be found in ref 5. We also used a sheet of PP sample (thickness 1.6 mm) fabricated by cold rolling,[6] which is denoted as PP-CR. Amoco 5013 grade of PP with a melt flow index of 2.5 dg/min was used to fabricate this specimen; no processing details were available.

Sample Characterization. All the PP samples used in our study were semicrystalline. The average heat of fusion measured by DSC at a heating rate of 20 °C /min for the samples was 105 ± 7 J/g. Although this indicates that there are some differences in crystallinity among the specimens, we did not specifically consider the degree of crystallinity in our results and discussion since the Brillouin measurements are averaged over both crystalline and amorphous regions of the specimen, as discussed below.

The refractive index (in the film plane and thickness direction) was measured using an Abbe refractometer with a

† Work done at Amoco Chemicals New Business R&D, Naperville, IL 60566.

10.1021/ma9906579 CCC: $19.00
Published on Web 02/05/2000

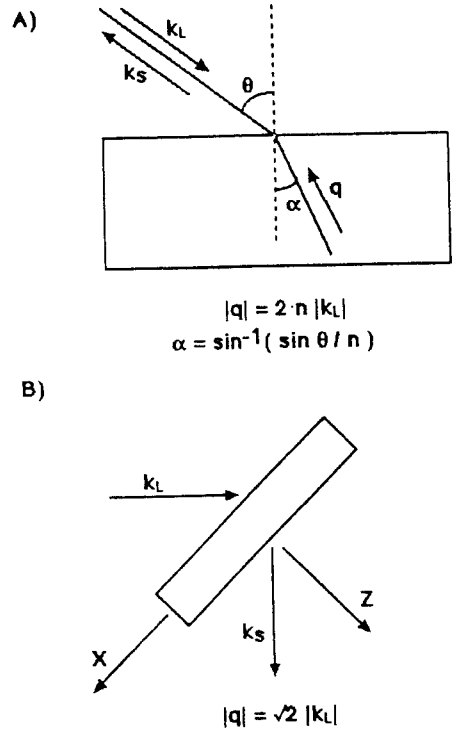

Figure 1. Scattering geometries used in Brillouin scattering experiments: (A) backscattering and (B) platelet. $\mathbf{k}_L$, $\mathbf{k}_s$, and $\mathbf{q}$ are the incident, scattered, and phonon wave vectors, respectively, and $k_L = 2\pi/\lambda_L$, where λ_L is the wavelength of the laser radiation.

rotatable polarizer mounted on the eyepiece. Measurements were made at 589.5 nm, with sample and prisms maintained at 20 °C (controlled by thermostatic water circulation). As remarked earlier, the PP specimens used here were produced with processing techniques capable of imparting substantial amount of molecular orientation, but no commensurate change in the enthalpy of fusion was recorded for these specimens by DSC. Such a trend showing no significant changes in density or degree of crystallinity accompanying drawing processes has also been reported by others.[18] We therefore used a density value of 0.906 g/mL (as reported by Amoco) for all specimens.

Brillouin Spectroscopy. The elastic symmetry exhibited by the sample and the associated elastic constants were determined through Brillouin spectroscopic measurements. Brillouin scattering is the inelastic scattering of light by acoustic phonons. An incident photon creates or annihilates a phonon, which results in a change in the frequency of the scattered light. These small frequency changes, detected by a Fabry-Perot interferometer, combined with the wavevector of the scattering process (the latter determined by the scattering geometry) allow the velocity of sound to be extracted. Details of the technique and the apparatus are described in ref 7. In order for Brillouin scattering to be effective, the medium must be homogeneous on the scale of the wavelength of light; in most cases a transparent material is a sufficient guarantee of this requirement. In the case of our samples the Brillouin technique measures the elastic response averaged over crystalline (many crystallites) and amorphous regions. In the context of the relation between polymer orientation and elastic properties, "polymer alignment" must be interpreted as an average over equivalent length scales (i.e., ~500 nm).

The scattering geometries used in this study are shown in Figure 1. In the backscattering geometry (Figure 1A), phonons with wavevector $q = 2nk_L$ (where n is the refractive index and k_L is the magnitude of the wavevector of the incident light) propagating close to the film normal can be probed. The angular dependence of the phonon velocity in the backscattering geometry was achieved by tilting the sample (i.e., changing θ in Figure 1A) with respect to the propagation axis of the light. In the platelet geometry (Figure 1B), phonons with $q = \sqrt{2}k_L$ propagating in the film plane along the x-axis are investigated. The angular dependence of the in-plane velocity was investigated by rotating the sample about the film normal (z-axis in Figure 1B). A variant of the platelet geometry was obtained by rotating the film by 45° with respect to the x-axis to gain additional information.

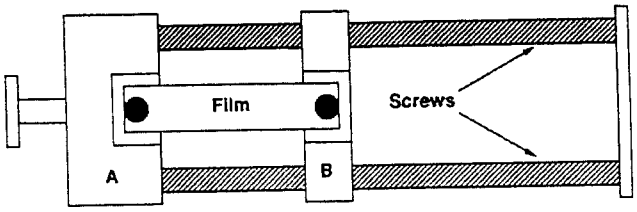

Figure 2. Schematic diagram of the stretching device.

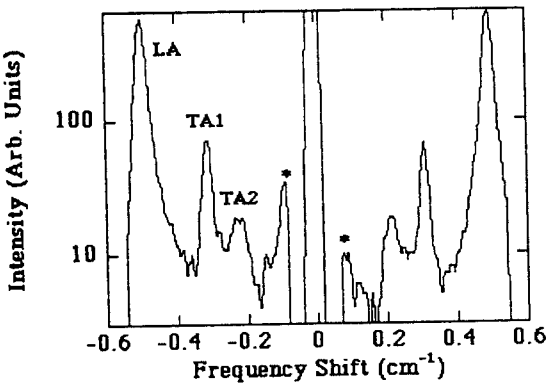

Figure 3. Typical Brillouin spectrum of polypropylene. LA and TA denote the longitudinal acoustic and transverse acoustic phonon, respectively. The features indicated by an asterisk are of instrumental origin.

To further investigate the dependence of film properties on molecular orientation, the sound velocities in uniaxially stretched PP-BIAX films (i.e., PP-BIAX was stretched along the two orthogonal axes in the film plane) were also measured. The stretching device, schematically shown in Figure 2, consists of a stationary piece A and a moving piece B. The test specimen (a strip of film ~5 cm by ~0.5 cm) is mounted firmly between pieces A and B. The strain induced in the test specimen upon manually turning the handle (which drives the micrometer screws) was tracked by measuring, with a traveling microscope, the change in spacing between two reference marks made on the film. The stretching was done in discrete steps (since the device was manually driven, no steady stretching rate was used) at room temperature, with care taken to avoid specimen slippage or slack. The experiment was terminated when the specimen failed ultimately with progressive load increase.

Piezobirefringence Measurements. Piezobirefringence characterizes the change in refractive index produced in a medium as a result of externally applied stresses or strains.[17] The stretching device shown in Figure 2, which could conveniently be mounted on the polarization stage of a microscope, was used for piezobirefringence measurements made at room temperature using the compensator method.[8] Monochromatic light (520 nm) from a xenon arc lamp was used for this purpose.

III. Results: As-Prepared Films

A Brillouin spectrum for polypropylene showing one longitudinal (LA) and two transverse (TA1 and TA2) phonons is given in Figure 3. (The peaks marked with asterisks are experimental artifacts caused by the insertion and removal of a filter that attenuates the intense central component.) The Brillouin frequency

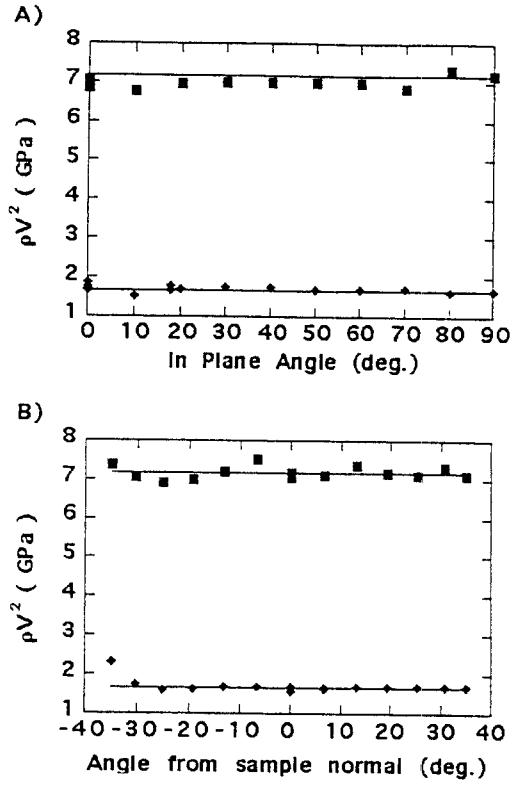

Figure 4. Elastic constants of PP-COMP measured in platelet (A) and backscattering (B) geometries. Solid squares and diamonds correspond to experimental longitudinal acoustic and transverse acoustic phonons, respectively. The lines represent the curve fits used to determine the C_{ij} in Table 1.

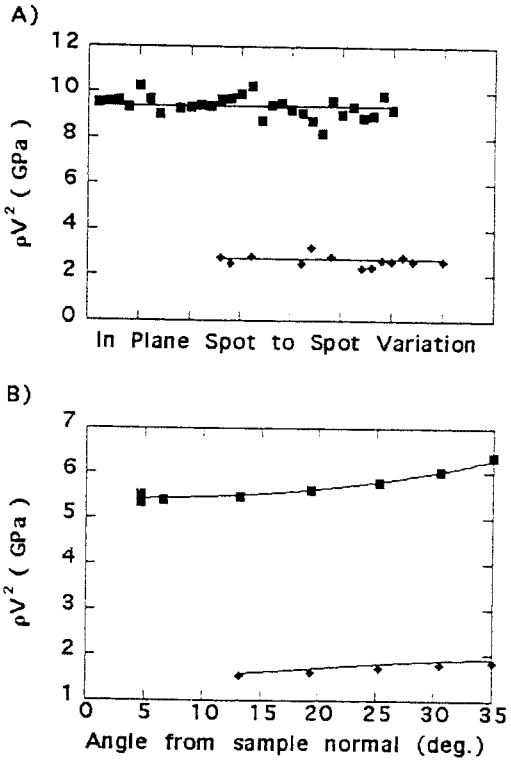

Figure 5. Elastic constants of PP-A0(X) measured in platelet (A) and backscattering (B) geometries. Solid squares and diamonds correspond to experimental longitudinal acoustic and transverse acoustic phonons, respectively. The lines represent the curve fits used to determine the C_{ij} in Table 1.

shifts are related to the acoustic phonon velocities (v_q) by

$$\Delta\omega = qv_q \tag{1}$$

where q is the wavevector appropriate for each scattering geometry as discussed above. The elastic constant (C_q) can then be calculated from $C_q = \rho v_q^2$ where ρ is the density. The determination of which particular element in the C_{ij} matrix[9] contributes to C_q involves both symmetry arguments and the specific experimental geometry employed.

Because we are dealing with polypropylene samples that are both semicrystalline and polycrystalline, the symmetry of the elastic constant tensor needs to be established for each sample prior to any quantitative analysis of the Brillouin data. This has been done through the determination of the angular dependence of the Brillouin frequencies. Birefringence was also used in the determination of the in-plane symmetry. When an anisotropic polymer film is observed through crossed polaroids, two orientations of the film produce extinction. Since these two axes are likely to coincide with the symmetry directions of elastic properties, they can be used as a guide for elastic measurements. When clear extinction directions were observed, we measured the angular dependence of the in-plane Brillouin frequencies with respect to one of these axes. For the PP-COMP, PP-A0(X), PP-A1(11), PP-A1(26), and PP-CR samples no extinction axes were present. In these cases the in-plane Brillouin frequencies were measured with respect to an arbitrary axis or to the fabrication machine direction if known. The PP-BIAX and PP-6X samples show clear extinction axes that coincide with the extrusion direction.

In Figure 4 we show the angular dependence of the Brillouin frequencies for PP-COMP measured in platelet (A) and backscattering (B) geometries (see Figure 1 and its description given in the Experimental Section). The observed phonon frequencies do not exhibit any angular dependence in or out of film plane. This behavior corresponds to an isotropic elastic symmetry for PP-COMP, consistent with the fact that no preferential molecular orientation is imparted during compression molding.

Plots for one of the forged samples, PP-A0(X), are shown in Figure 5. The upper part corresponds to the platelet geometry and gives the in-plane velocity. Because the in-plane birefringence showed very large inhomogeneities, we probed the in-plane velocity as a function of position on the film (Figure 5A). The resulting large spread in the elastic response precluded an accurate angular study of the in-plane velocities. The backscattering data, on the other hand (Figure 5B), show discernible angular dependence in the out-of-plane phonon behavior. Based on Figure 5A,B the overall behavior of this particular forged sample corresponds to hexagonal elastic symmetry.

The behavior of the other two forged samples, PP-A1(11) and PP-A1(26), is depicted in Figures 6 and 7, respectively. From the platelet geometry results (Figures 6A and 7A), we see that PP-A1(11) exhibits weak anisotropic behavior in the film plane, whereas PP-A1(26) is distinctly anisotropic in-plane. The out-of-plane behavior (Figures 6B and 7B) of both these samples is clearly anisotropic. Because of the in-plane anisotropy, backscattering data have been measured for two orthogonal tilts denoted by the full and open symbols. These two sets of backscattering data allow us to extract a more complete set of elastic constants.

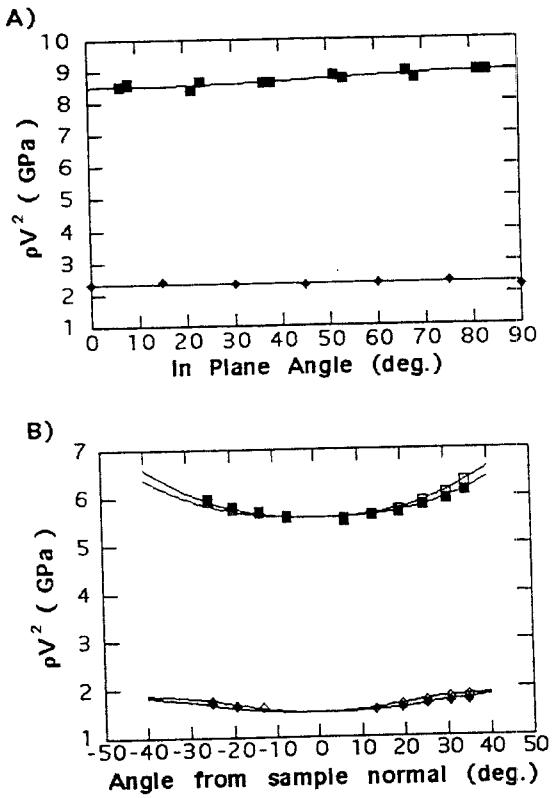

Figure 6. Elastic constants of PP-A1(11) measured in platelet (A) and backscattering (B) geometries. Squares and diamonds correspond to experimental longitudinal acoustic and transverse acoustic phonons, respectively; in (A) they correspond to values in the $X-Y$ plane, in (B) the solid symbols are for the $Z-Y$ plane and the open symbols are for the $Z-X$ plane. The lines represent the curve fits used to determine the C_{ij} in Table 1.

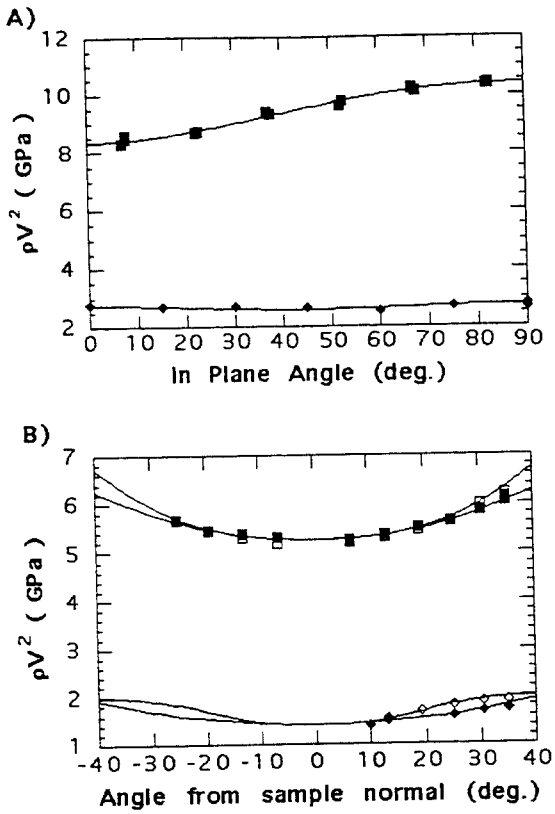

Figure 7. Elastic constants of PP-A1(26) measured in platelet (A) and backscattering (B) geometries. Squares and diamonds correspond to experimental longitudinal acoustic and transverse acoustic phonons, respectively; in (A) they correspond to values in the $X-Y$ plane, in (B) the solid symbols are for the $Z-Y$ plane and the open symbols are for the $Z-X$ plane. The lines represent the curve fits used to determine the C_{ij} in Table 1.

The plots for the PP-BIAX, PP-6X, and PP-CR samples are shown in Figures 8, 9, and 10, respectively. The overall behavior of these samples is similar to those in Figures 6 and 7 except that the anisotropies are considerably larger. The elastic symmetry compatible with the results in Figures 6–10 is clearly lower than hexagonal. Noting the mirror symmetry with respect to the z-axis in the backscattering data, and 180° repeat patterns in the in-plane behavior, we conclude that the A1(11), A1(26), BIAX, CR, and 6X films all have orthorhombic symmetry.

Determination of the elastic symmetry of the films allows us to know the corresponding number of independent elastic constants to be determined from Brillouin frequency shifts. The C_{ij} matrix for an orthorhombic system[9] is

$$\begin{matrix} C_{11} & C_{12} & C_{13} & 0 & 0 & 0 \\ C_{12} & C_{22} & C_{23} & 0 & 0 & 0 \\ C_{13} & C_{23} & C_{33} & 0 & 0 & 0 \\ 0 & 0 & 0 & C_{44} & 0 & 0 \\ 0 & 0 & 0 & 0 & C_{55} & 0 \\ 0 & 0 & 0 & 0 & 0 & C_{66} \end{matrix}$$

with nine independent elements, and the number of independent elements for a hexagonal system reduces to five, since $C_{11} = C_{22}$, $C_{13} = C_{23}$, $C_{44} = C_{55}$ and $C_{66} = (C_{11} - C_{12})/2$. For isotropic systems the number of independent elastic constants is two, since $C_{11} = C_{22} = C_{33}$, $C_{12} = C_{23} = C_{13}$, $C_{44} = C_{55} = C_{66}$ and $C_{11} - C_{12} = 2C_{44}$.

The elastic constants calculated from the least-squares fitting of the Brillouin data are given in Table 1 together with their estimated uncertainties. The full lines in Figures 4–10 are the values of ρV^2 calculated using the C_{ij} in Table 1, and clearly they provide an excellent description of the elastic response of the films. For the sake of completeness, we have listed in Table 2 the elastic compliance constants (S_{ij}) obtained by inverting the C_{ij} tensor.

It should be noted that we chose our coordinate axes with the 3(z)-axis along the film normal. The assignment of the in-plane 1 and 2 (x and y) axes was made after completion of the Brillouin measurements so that C_{11} was greater than C_{22}.

IV. Discussion

The elastic constants calculated from Brillouin measurements, collected in Tables 1 and 2, bring out certain interesting trends. First of all, it is seen that the elastic symmetry, determined using Brillouin scattering, depends on the particular film fabrication technique employed. Thus, the compression molding of PP-COMP, which involves little molecular orientation during processing, produces isotropic elastic symmetry. A priori we expected the PP-A0(X), -A1(11), and -A1(26) samples to exhibit hexagonal symmetry since they all were fabricated using uniaxial compression processes expected to impart a true biaxial deformation to the film plane.[9] Contrary to this expectation, we find different degrees of in-plane anisotropy in the various films

Table 1. Elastic Stiffness Constants (GPa) of PP Films

C_{ij} (GPa)	COMP	BIAX	6X	A0(X)	A1(11)	A1(26)	CR
C_{11}	7.16 ± 0.07	12.2 ± 0.5	16.9 ± 0.5	9.4 ± 0.05	8.96 ± 0.36	10.4 ± 0.42	9.19 ± 0.38
C_{22}	7.16 ± 0.07	7.58 ± 0.3	5.37 ± 0.20	9.4 ± 0.05	8.50 ± 0.35	8.36 ± 0.37	7.25 ± 0.32
C_{33}	7.16 ± 0.07	5.65 ± 0.05	5.63 ± 0.11	5.42 ± 0.06	5.57 ± 0.10	5.26 ± 0.04	5.86 ± 0.10
C_{44}	1.67 ± 0.02	1.25 ± 0.15	1.14 ± 0.04	1.49 ± 0.10	1.40 ± 0.05	1.41 ± 0.06	1.55 ± 0.14
C_{55}	1.67 ± 0.02	1.5 ± 0.1	1.84 ± 0.07	1.49 ± 0.10	1.50 ± 0.05	1.35 ± 0.06	1.59 ± 0.06
C_{66}	1.67 ± 0.02	2.77 ± 0.15	1.76 ± 0.04	2.7 ± 0.2	2.31 ± 0.16	2.74 ± 0.16	2.19 ± 0.11
C_{12}	3.82 ± 0.11	3.83 ± 0.17	3.23 ± 0.21	4.0 ± 0.5	4.06 ± 0.26	4.13 ± 0.29	3.15 ± 0.13
C_{13}	3.82 ± 0.11	3.33 ± 0.07	3.33 ± 0.19	3.18 ± 0.25	3.26 ± 0.06	3.24 ± 0.05	3.16 ± 0.07
C_{23}	3.82 ± 0.11	3.46 ± 0.30	3.63 ± 0.08	3.18 ± 0.25	3.23 ± 0.06	3.22 ± 0.05	3.05 ± 0.10

Table 2. Elastic Compliance Constants (10^{-10} m^2/N) of PP Films

S_{ij}	COMP	BIAX	6X	A0(X)	A(11)	A1(26)	CR
S_{11}	2.2 ± 0.1	1.0 ± 0.1	0.69 ± 0.02	1.4 ± 0.01	1.6 ± 0.08	1.3 ± 0.06	1.4 ± 0.07
S_{22}	2.2 ± 0.1	1.9 ± 0.1	3.4 ± 0.2	1.4 ± 0.01	1.7 ± 0.09	1.7 ± 0.1	1.9 ± 0.1
S_{33}	2.2 ± 0.1	2.6 ± 0.02	3.2 ± 0.2	2.6 ± 0.04	2.5 ± 0.06	2.7 ± 0.03	2.4 ± 0.06
S_{44}	6.0 ± 0.7	8.0 ± 0.8	8.8 ± 0.3	6.7 ± 0.4	7.1 ± 0.2	7.1 ± 0.3	6.4 ± 0.5
S_{55}	6.0 ± 0.7	6.7 ± 0.5	5.4 ± 0.2	6.7 ± 0.4	6.7 ± 0.2	7.4 ± 0.3	6.3 ± 0.2
S_{66}	6.0 ± 0.7	3.6 ± 0.1	5.7 ± 0.1	3.7 ± 0.3	4.3 ± 0.6	3.7 ± 0.2	4.6 ± 0.2
S_{12}	−0.77 ± 0.06	−0.34 ± 0.03	−0.25 ± 0.07	−0.41 ± 0.1	−0.52 ± 0.08	−0.42 ± 0.1	−0.37 ± 0.04
S_{13}	−0.77 ± 0.06	−0.40 ± 0.02	−0.25 ± 0.05	−0.61 ± 0.1	−0.62 ± 0.03	−0.51 ± 0.05	−0.57 ± 0.03
S_{23}	−0.77 ± 0.06	−1.0 ± 0.1	−0.20 ± 0.2	−0.61 ± 0.1	−0.67 ± 0.03	−0.78 ± 0.02	−0.77 ± 0.05

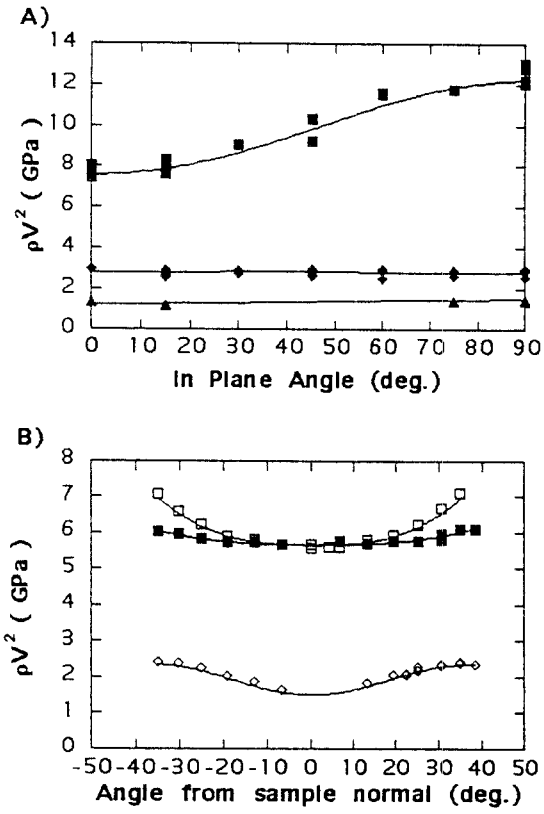

Figure 8. Elastic constants of PP-BIAX measured in platelet (A) and backscattering (B) geometries. Squares correspond to experimental longitudinal acoustic phonons. Diamonds and triangles correspond to experimental transverse acoustic phonons. In (A) they correspond to values in the $X-Y$ plane. In (B) the solid symbols are for the $Z-Y$ plane and the open symbols are for the $Z-X$ plane. The lines represent the curve fits used to determine the C_{ij} in Table 1.

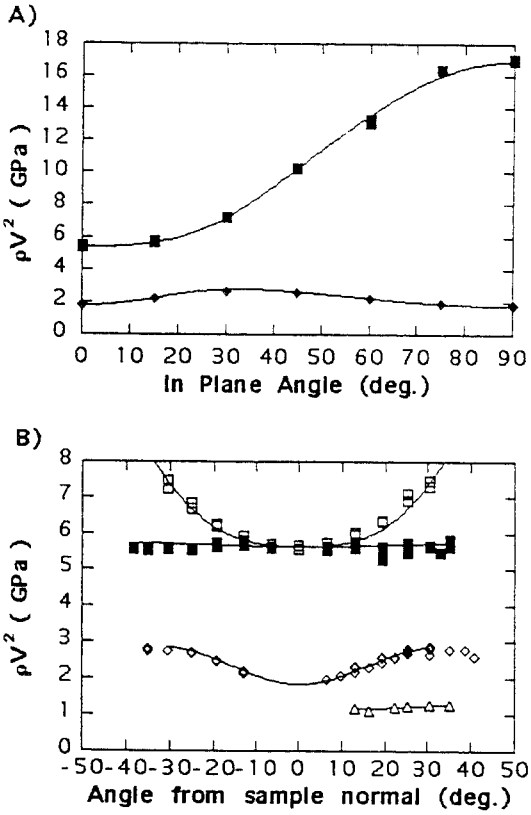

Figure 9. Elastic constants of PP-6X measured in platelet (A) and backscattering (B) geometries. Squares correspond to experimental longitudinal acoustic phonons. Diamonds and triangles correspond to experimental transverse acoustic phonons. In (A) they correspond to values in the $X-Y$ plane. In (B) the solid symbols are for the $Z-Y$ plane and the open symbols are for the $Z-X$ plane. The lines represent the curve fits used to determine the C_{ij} in Table 1.

ranging from isotropic (PP-A0(*X*)) to anisotropic (PP-A1(26)). We interpret this as an indication that the biaxial fabrication techniques must be dependent on subtle, and as yet uncontrolled, parameters. This trend is consistent with the optical characterization studies on similar forged films reported by Osawa et al.[10,11] The in-plane anisotropy exhibited by PP-BIAX also indicates unequal molecular orientation resulting from the fabrication technique. This is consistent with the traditional industrial practice of using biaxial stretching to achieve the desired balance in mechanical properties, whether or not the fabrication process results in perfect biaxiality. The cold rolled sample (PP-CR) was expected to have orthorhombic symmetry since all three axes are inequivalent during fabrication;[6,19] indeed this was found to be the case. Interestingly, although similar arguments can be made for PP-6X, it can be seen from Table 1 that the C_{22} and C_{33} values for PP-6X are equal

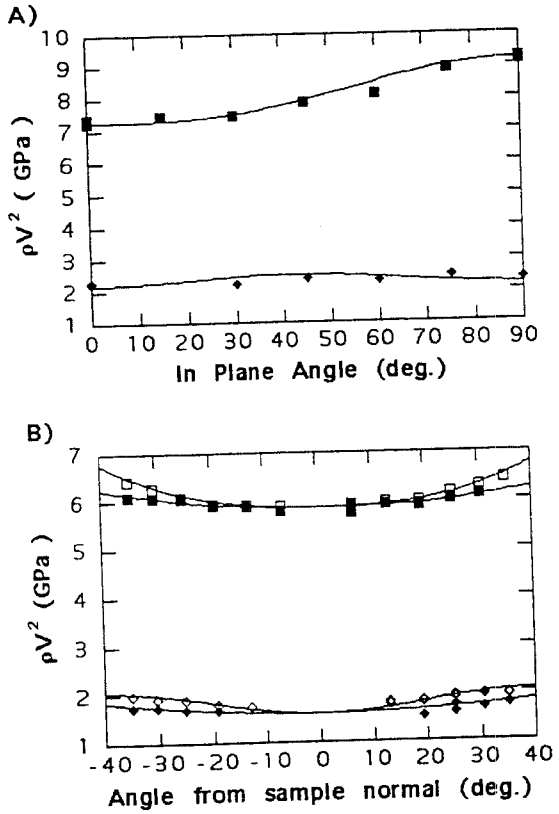

Figure 10. Elastic constants of PP-CR measured in platelet (A) and backscattering (B) geometries. Squares and diamonds correspond to experimental longitudinal acoustic and transverse acoustic phonons, respectively; in (A) they correspond to values in the $X-Y$ plane, in (B) the solid symbols are for the $Z-Y$ plane and the open symbols are for the $Z-X$ plane. The lines represent the curve fits used to determine the C_{ij} in Table 1.

within the experimental error. This indicates that the axis of symmetry is no longer the surface normal but the stretch direction during fabrication. This is not a surprise, since it is well documented that uniaxially extruded profiles (strands, rods, and fibers) exhibit isotropy transverse to the draw direction.[12]

Other general trends shown by the data in Table 1 are (i) the largest compressional constant (C_{ii}) is always along the machine draw direction during fabrication, (ii) the compressional elastic constant in the transverse directions are always substantially smaller, (iii) the longitudinal constant along the surface normal (C_{33}) is quite insensitive to the fabrication process, (iv) all shear-related constants, C_{44}, C_{55}, and C_{66} (S_{44}, S_{55}, and S_{66}), are considerably smaller (larger) than their corresponding compressional counterparts.

Since polymers are known to be "strong" along the chain direction and "weak" perpendicular to the chains where only van der Waals forces play a role, we may expect any preferential polymer orientation to be the "strongest" direction in the film. Items i, ii, and iv above can be rationalized on the basis that the polymer molecular alignment occurs along the machine draw direction during processing. Item iii can be interpreted as an indication that the polymer chains tend to align in the plane of the films. The variations in the C_{11} values shown in Table 1 thus reflect the different extents to which the molecular orientation has been imparted by the processing technique in the plane of the film. For example, consistent with the nature of processing and

Table 3. Comparison Between Calculated Reuss and Voigt Averaging of PP-6X Films and Measured Elastic Constants of PP-COMP (10^{-10} m²/N)

	S_{11}	S_{44}
Reuss PP-6X	3.0	8.3
Voigt PP-6X	2.1	5.6
PP-COMP	2.2	6.0

the corresponding isotropic elastic symmetry, the compression molded specimen, PP-COMP, gives the lowest value for C_{11}, whereas PP-6X, having the highest degree of uniaxial orientation, exhibits the highest C_{11} value.

To correlate the elastic constants measured by Brillouin scattering (C_{ij}) with molecular structure and morphology and also with other elastic moduli used in applications, it is often simpler to use the compliance constants (S_{ij}) given in Table 2. For example, Young's moduli, (E_i; the ratio of applied stress along the i direction to strain along the same axis) and Poisson's ratios (ν_{ij}; the ratio of the contraction along the j direction to the extension along the i direction produced by a uniaxial stress along the i direction) can be related to the elastic compliance constants in a straightforward fashion. For a specimen possessing orthorhombic symmetry the often-used moduli can be written:

$$E_1 = 1/S_{11} \qquad E_2 = 1/S_{22} \qquad E_3 = 1/S_{33} \tag{2}$$

$$G_1 = C_{44} = 1/S_{44} \qquad G_2 = C_{55} = 1/S_{55} \qquad G_3 = C_{66} = 1/S_{66} \tag{3}$$

$$\nu_{12} = -(S_{12}/S_{11}) \qquad \nu_{13} = -(S_{13}/S_{11})$$
$$\nu_{23} = -(S_{23}/S_{22}) \qquad \nu_{21} = -(S_{12}/S_{22}) \tag{4}$$
$$\nu_{31} = -(S_{13}/S_{33}) \qquad \nu_{32} = -(S_{23}/S_{33})$$

The above trends can be qualitatively understood in the framework of theoretical models developed to understand the origin and development of mechanical anisotropy,[13] the simplest of which is Ward's aggregate model.[14] According to this model, the polymer can be considered as an aggregate of identical units that, in the unstretched state, are oriented randomly. As the material is stretched uniaxially, these aggregates tend to align with the draw direction. (An affine response to deformation of aggregates is assumed.) Although developed for oriented fibers, the applicability of this model may be tested for uniaxially oriented films. The ideas behind Ward's model[14] can be tested in a more quantitative manner by noting that if the changes in elastic properties are due only to reorientation of domains, then the elastic constants of "ordered" and "random" samples should be related. If one were to imagine breaking up an anisotropic sample and then randomly reassembling the pieces, the C_{ij} of the reconstituted (isotropic) sample should be an average of the original C_{ij}. The exact averaging procedure is still not known, but two averaging procedures exist that, because of their mathematical simplicity, are often used: these are the Voigt and Reuss averages.[14] It can be shown that these averages represent the maximum or minimum values for all other averaging procedures. In Table 3 we have listed the Voigt and Reuss averages of the elastic constants of PP-6X and compare them with those measured for PP-COMP, which exhibits isotropic symmetry. The measured values lie within the bounds predicted by the two averaging schemes, indicating that

the Ward model provides a reasonable description of how domain orientation plays a major role in determining mechanical properties.

V. Relation Between Molecular Orientation and Properties

One attempt to quantitatively correlate elastic and molecular orientation was proposed by Moseley.[15] He empirically related the sound velocity (v) to Hermann's orientation parameter[16] f as

$$f \equiv \langle 3\cos^2\beta - 1\rangle/2 = 1 - (v_0/v)^2 \qquad (5)$$

where v_0 is the sound velocity for no preferential orientation, i.e. $f = 0$, and β is the angle between the polymer chains and the propagation direction. This approach suffers from a few drawbacks: the orientation parameter is appropriate only for uniaxial cases (which lead to hexagonal symmetry), and eq 5 predicts an infinite velocity for a perfectly aligned material ($\cos^2\beta = 1$), which is unphysical.

Here we propose an alternative definition of "orientation" parameters and show that they can be easily related to both the elastic and optical properties of the materials investigated. Let each polymer chain (or equivalently each Ward domain) be characterized by its three direction cosines (β_i). We define

$$f_i = \langle\cos^2(\beta_i)\rangle \qquad (6)$$

as the three orientation parameters; note that, by definition, $f_1 + f_2 + f_3 = 1$ so that f_i can be regarded as the probability that a chain (or domain) is aligned along axis i. In this scheme ($f_1 = 1, f_2 = f_3 = 0$), ($f_1 = 0, f_2 = f_3 = {}^1/_2$), and ($f_1 = f_2 = f_3 = {}^1/_3$) correspond to uniaxially aligned, biaxially aligned, and randomly aligned chains/domains, respectively. When the chains or domains are endowed with anisotropic optical and elastic properties, it follows that the birefringence is expected to be of the form

$$n_i - n_j = K(f_i - f_j) \qquad (7)$$

where K is a phenomenological parameter related to the optical anisotropy of the domains. Similarly, the elastic properties may be expected to be of the form

$$\begin{aligned} S_{11} &= f_1 S_{\parallel} + (f_2 + f_3) S_{\perp} \\ S_{22} &= f_2 S_{\parallel} + (f_1 + f_3) S_{\perp} \\ S_{33} &= f_3 S_{\parallel} + (f_1 + f_2) S_{\perp} \end{aligned} \qquad (8)$$

where $S_{\parallel}$ and $S_{\perp}$ are the elastic compliance constants of the individual domains (chains) parallel and perpendicular to the orientation axis. Similar equations can be written for the other S_{ij}'s, but since they appear to be less sensitive to processing (Table 2), they are likely to be less significant and will not be considered here.

The measured refractive indices for PP-6X are $n_x = 1.535$, $n_y = 1.496$, and $n_z = 1.496$. Using eq 7, we obtain $f_2 = f_3$ and $K = 0.039/(f_1 - f_2)$. Although we cannot solve for all parameters, it seems reasonable with our present knowledge to assume a high degree of alignment in the PP-6X sample: for the sake of example we assume $f_1 = 1$. This approximation then yields $K = 0.039$. The same approximation and eqs 8 yield $S_{\parallel} = 0.069$ and $S_{\perp} = 0.33$ GPa^{-1}. The validity of the model must now be tested as

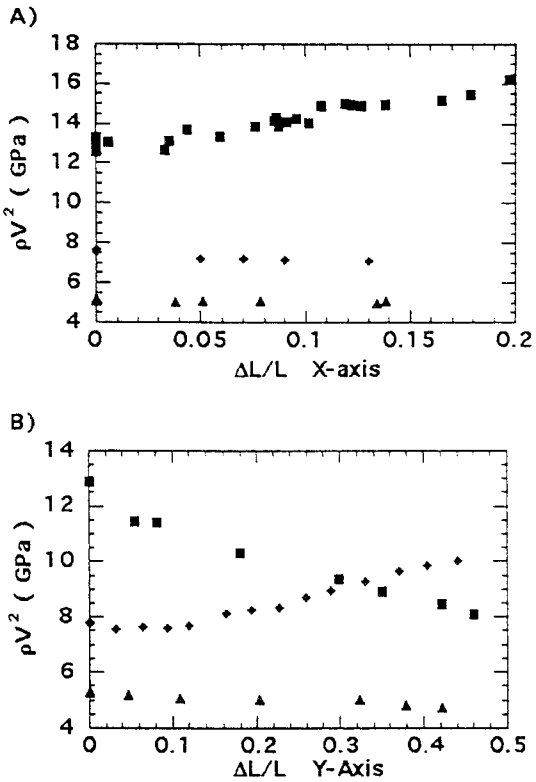

Figure 11. Variation in elastic constants (C_{11}, squares; C_{22}, diamonds; C_{33}, triangles) with stretching of PP-BIAX film: along x-axis (A) and along y-axis (B).

to how well the above parameters (which are extracted only from the PP-6X sample) describe the other samples.

PP-COMP is not birefringent, and hence eq 7 requires that $f_1 = f_2 = f_3 = {}^1/_3$. Equations 8 then predict $S_{11} = 2.2$, in excellent agreement with the measured value. For PP-BIAX the measured refractive indices are 1.518, 1.508, and 1.500 which, combined with eq 7, yield $f_1 = 0.57$, $f_2 = 0.32$, and $f_3 = 0.11$. Equations 8 then yield $S_{11} = 1.4$, $S_{22} = 2.3$, and $S_{33} = 2.9$. The trend $S_{11} < S_{22} < S_{33}$ is well reproduced by the model, but the numerical values are as much as 40% different from the measured values (Table 2). Given the approximations made, we feel that this is still a satisfactory agreement.

VI. Results and Discussion: Stretched Films

To further illustrate how the Brillouin scattering technique can be used to track the changes induced by sample processing, we carried out Brillouin spectroscopic measurements on uniaxially stressed PP-BIAX films using the device shown in Figure 2. The uniaxial stretching was performed at room temperature along both x- and y-axes (orthogonal to each other) in the plane of the film. Brillouin shifts due to changes in the corresponding phonon velocities were tracked as a function of stretching. The corresponding variation in the elastic constants C_{11}, C_{22}, and C_{33} with stretching along the x- and y-axis are presented in Figure 11. The measurements were made until failure occurred. Upon stretching along the x-axis (Figure 11A), C_{11} increases, C_{22} decreases slightly, and C_{33} remains virtually unaffected. Upon stretching along the y-axis (see Figure 11B), C_{11} decreases, C_{22} increases, and C_{33} remains unaffected.

The piezobirefringence results for the same material are shown in Figure 12, where the measured in-plane birefringence, $n_x - n_y$, is plotted as a function of strain

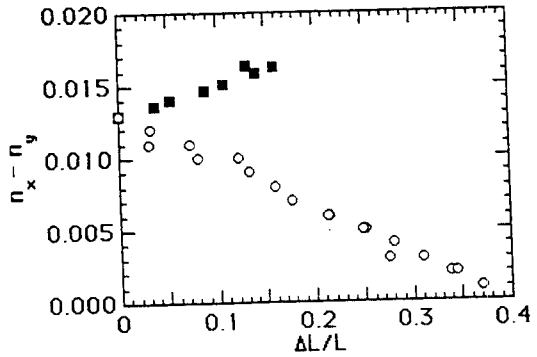

Figure 12. Variation of in-plane birefringence with stretching of PP-BIAX film: along x-axis (solid squares) and y-axis (open circles).

along the x- and y-axis in the plane of the film. In terms of the model presented in the previous section, the birefringence results for an x-strain indicate an increase in f_1 and a decrease in f_2, which, in turn, through eqs 8 translate into an increase in C_{11} and a decrease in C_{22}, in agreement with the observation (as shown in Figure 11). Conversely, the y-strain birefringence results indicate an increase in f_2 and a decrease in f_1, which, in turn, through eqs 8 translate into an increase in C_{22} and a decrease in C_{11}, also in agreement with the observed trend in Brillouin measurements. Also notable is that the birefringence is zero at a y-strain of 0.38, indicating that $f_1 = f_2$ and consequently that $C_{11} = C_{22}$. From Figure 11 we see that $C_{11} = C_{22}$ at a strain of 0.32, which is in fair agreement with the value (0.38) corresponding to zero birefringence seen in Figure 12.

VII. Conclusion

Elastic properties of polypropylene films obtained by several common processing techniques have been determined using Brillouin scattering techniques. We have shown that the elastic symmetry and the corresponding elastic constants obtained through Brillouin spectroscopic measurements are clearly dependent on the molecular orientation present in the films, brought about by the various processing techniques. The uniaxially stretched film specimen, PP-6X, exhibits hexagonal symmetry, with isotropic properties transverse to the orientation axis, similar to oriented fibers. We find that Ward's aggregate model, combined with a modified definition of molecular alignment, allows birefringence and elastic data to be directly related to molecular orientation.

We have shown that Brillouin scattering techniques can successfully be used to track the molecular orientation induced by uniaxial stretching. We find a correspondence between the Brillouin measurements and optical birefringence measurements, again illustrating that molecular orientation plays a dominant role in determining the mechanical anisotropy of polymer films.

Acknowledgment. We thank Amoco's new business development department for the support of this work. The work at Argonne National Labs was done under DOE Contract W-31-109-ENG-38. We thank Costas Metaxas and Beverley Holze (Amoco) for the refractive index measurements. Terre Van Kirk of Amoco prepared PP-COMP specimens. We also thank Prof. Roger Porter of University of Massachusetts for kindly supplying the forged PP samples used in this study and dedicate this paper to his memory.

References and Notes

(1) Ward, I. M. In *Structure and Properties of Oriented Polymers*; Ward, I. M., Ed.; Applied Science: London, 1975; Chapter 1.
(2) Holliday, L. In *Structure and Properties of Oriented Polymers*; Ward, I. M., Ed.; Applied Science: London, 1975; p 244.
(3) Treloar, L. R. G. *Plast. Polym.* **1970**, *39*, 29.
(4) Samuels, R. J. *J. Polym. Sci., Part A-2* **1965**, *3*, 1741.
(5) Saraf, R. F.; Porter, R. S. *J. Rheol.* **1987**, *31*, 59.
(6) Moore, E. P. In *Polypropylene Handbook*; Moore, E. P., Ed.: Hanser: New York, 1996; Chapter 9; *Plast. Des. Process.* **1971**, *11*, 24.
(7) Kumar, S. S.; Fartash. A.; Grimsditch, M.; Schuller, I. K.: Kumar, R. S. *Macromolecules* **1993**, *26*, 6184.
(8) Hartshorne, N. H.; Stuart, A. *Crystals and the Polarizing Microscope*; Elsevier: New York, 1970.
(9) Love, A. E. H. *A Treatise on the Mathematical Theory of Elasticity*, 4th ed.; Macmillan: New York. 1944.
(10) Osawa, S.; Porter, R. S. *Polymer* **1994**, *35*, 540.
(11) Osawa, S.; Porter, R. S.; Ito, M. *Polymer* **1994**, *35*, 551.
(12) Hadley, D. W.; Pinnock, P. R.; Ward, I. M. *J. Mater. Sci.* **1969**, *4*, 152.
(13) Hadley, D. W.; Ward, I. M. In *Structure and Properties of Oriented Polymers*; Ward, I. M., Ed.; Applied Science: London, 1975; Chapter 8.
(14) Ward, I. M. *Proc. Phys. Soc.* **1962**, *80*, 1176.
(15) Moseley, W. W., Jr. *J. Appl. Polym. Sci.* **1960**, *3*, 266.
(16) Hermanns, P. H. *Physics and Chemistry of Cellulose Fibers*; Elsevier: New York, 1949; pp 230–4.
(17) Nye, J. F. *Physical Properties of Crystals*; Clarendon: Oxford, 1964.
(18) Wang, C. H.; Cavanaugh, D. B. *J. Appl. Phys.* **1981**, *52*, 6003; *Macromolecules* **1981**, *14*, 1061.
(19) Wilchinsky, Z. W. *J. Appl. Polym. Sci.* **1963**, *7*, 923.

MA9906579